

Voltage window for sustained elevation of cytosolic calcium in smooth muscle cells

(calcium channels/window currents/inactivation/membrane potential)

BERND K. FLEISCHMANN*, RICHARD K. MURRAY†, AND MICHAEL I. KOTLIKOFF*†‡

*Department of Animal Biology, School of Veterinary Medicine, and †Department of Medicine, School of Medicine, University of Pennsylvania, Philadelphia, PA 19104-6046

Communicated by Clay M. Armstrong, August 24, 1994 (received for review December 15, 1993)

ABSTRACT Action potentials activate voltage-dependent calcium channels and attendant increases in cytosolic calcium concentration ($[Ca^{2+}]_i$) in many excitable cells. The role of these channels in the regulation of $[Ca^{2+}]_i$ in nonspiking cells that do not depolarize to membrane potentials sufficient to activate a substantial fraction of the available current is less clear. Measurements of the peak activation and steady-state inactivation of L-type calcium currents have predicted the existence of a noninactivating current window over a voltage range where channel inactivation is incomplete. The degree to which such small currents might regulate $[Ca^{2+}]_i$, however, has not been established. Here we demonstrate a “calcium window” in nondialyzed, quiescent smooth muscle cells over a small voltage range near the resting membrane potential. Sustained depolarizations in this voltage range, but not to more positive potentials, resulted in sustained rises in calcium, despite the fact that macroscopic inward currents were <2 pA. The calcium window corresponded well with the predicted window current determined under the same conditions; the peak of the calcium window occurred at -30 mV, with steady-state rises in $[Ca^{2+}]_i$ in some cells at -50 mV. Steady-state rises in $[Ca^{2+}]_i$ following depolarization were completely blocked by nisoldipine and were augmented and shifted to more negative potentials by BAY K8644. Voltage-dependent calcium channels thus regulate steady-state calcium levels in nonspiking cells over a voltage range where macroscopic currents are only barely detectable. This voltage range is bounded at negative potentials by calcium channel activation and at more positive potentials by channel inactivation.

Activation of voltage-dependent, L-type calcium channels by action potentials contributes to the regulation of cytosolic calcium concentration ($[Ca^{2+}]_i$) in excitable cells that display spiking electrical activity (1–6). Increases in the frequency of action potentials in such cells increase $[Ca^{2+}]_i$, either as a direct result of the calcium transient or due to calcium-induced calcium release (3, 4, 7, 8–11). Calcium channels are present in many cells that do not demonstrate spiking electrical activity, however. Some smooth muscle cells, as well as nonexcitable cells such as fibroblasts, epithelial cells, and endocrine cells, display graded changes in membrane potential as well as tonic alterations in $[Ca^{2+}]_i$ that underlie sustained cellular responses (12–14). The membrane potential of these cells fluctuates but generally does not depolarize to potentials required to activate a substantial fraction of the available calcium current. Measurements of L-type calcium currents in a variety of cells have suggested that a theoretical “window current” of steady-state calcium flux exists (15–21). This prediction arises from the fact that a small amount of current is available over a negative voltage range at which steady-state current inactivation is incomplete. Measurements of sustained

currents of low amplitude have been reported under recording conditions of elevated divalent ion concentrations in several cell types (22–25), but the extent of current inactivation in such experiments depends largely on experimental conditions, particularly the degree of calcium-induced channel inactivation (6). Moreover, the degree to which such currents, which are at the threshold of detectability, result in increases in $[Ca^{2+}]_i$ has not been established. Recent evidence suggests that L-type calcium channel activity near the resting membrane potential may be an important regulator of cellular function (13, 26, 27), consistent with single-channel measurements indicating that calcium channel open-state probability is appreciable in physiological voltage ranges negative to the apparent threshold of the macroscopic current (28, 29). Here we use nondialyzed, quiescent airway myocytes to directly demonstrate the existence of a calcium window in the range of the physiological resting potential of nonspiking smooth muscle cells.

MATERIALS AND METHODS

Individual equine tracheal myocytes were dissociated and recorded at 35°C as described (30). Cells were loaded with fura-2 by incubation at 38°C in $2\ \mu\text{M}$ fura-2AM for 10–15 min, followed by a 20-min wash in extracellular solution (see below). We estimated the final intracellular concentration of fura 2 in our experiments as between 40 and $60\ \mu\text{M}$ by dialyzing cells with varying concentrations of fura-2 free acid and comparing fluorescence intensity at the isosbestic wavelength (357 nm) with that of fura-2AM-loaded cells. The loading medium consisted of (mM) NaCl, 115; glucose, 15; Hepes, 25; CaCl_2 , 2; KCl, 5; MgCl_2 , 1 (pH 7.4). Quantitative photometry was performed using a computer-controlled filter wheel (Metaltek) providing 340-nm and 380-nm excitation pairs at 2 Hz through a $40\times$ oil immersion lens (Nikon). Emitted fluorescence (510 nm), whole-cell currents, and command potential signals were simultaneously recorded on VCR tape using a four-channel PCM (Instrutech) and then deconvoluted and digitized off-line. Background fluorescence was estimated for each cell individually at the end of the experiment. Fura signals were calibrated following permeabilization by obtaining signals under saturating calcium conditions (2 or $10\ \text{mM}$ Ca^{2+}) and minimum calcium conditions (10-fold excess EGTA), and $[Ca^{2+}]_i$ was calculated by standard methods (31). Mean values for R_{\min} , R_{\max} , and $F_{380_{\max}}/F_{380_{\min}}$ were 0.35, 2.1, and 3.9, respectively; the K_d used was 386 nM (32). Cell currents were recorded using the nystatin modification (33) of the whole-cell patch-clamp method (34). Signals were amplified (Heka EPC-9), filtered at 2.3 kHz, and recorded to computer and VCR tape. Current traces recorded during sustained depolarizations were digitized from tape at 250 Hz and filtered at 100 Hz. Pipette solution was as follows (mM):

The publication costs of this article were defrayed in part by page charge payment. This article must therefore be hereby marked “advertisement” in accordance with 18 U.S.C. §1734 solely to indicate this fact.

Abbreviation: $[Ca^{2+}]_i$, cytosolic calcium concentration.
‡To whom reprint requests should be addressed.

cesium acetate, 80; CsCl, 50; MgCl₂, 5; EGTA, 3; CaCl₂, 1; Hepes, 10; and nystatin, 300 units/ml. Extracellular solution consisted of (mM) NaCl, 125; KCl, 5; MgCl₂, 1; Hepes, 10; CaCl₂, 1.8.

RESULTS AND DISCUSSION

To determine the degree to which calcium currents at or below the limit of resolution of the patch-clamp technique contribute to the regulation of steady-state $[Ca^{2+}]_i$ in non-spiking cells under physiologic conditions, measurements of $[Ca^{2+}]_i$ and current were made in nystatin-permeabilized tracheal smooth muscle cells that have graded electrical activity. Despite disadvantages associated with precise calcium quantification in fura-2AM-loaded cells (35, 36), this preparation enabled measurements under near physiological calcium buffering conditions (low fura concentration and nondialyzed endogenous buffers), which is required for the observation of relatively small rises in $[Ca^{2+}]_i$ (37), and allowed repeated long-duration voltage clamp experiments with minimal current rundown (33). Brief (250 ms) duration voltage-clamp steps to window current voltages (-25 to -40 mV) evoked little or no inward current and no rise in $[Ca^{2+}]_i$, whereas more positive steps that fully activated the current evoked a transient rise in $[Ca^{2+}]_i$ (Fig. 1A). Conversely, sustained depolarizations to the same potentials produced dramatically different calcium responses. Voltage-clamp steps to potentials within the predicted voltage range for calcium window currents led to a gradual rise in $[Ca^{2+}]_i$ that was sustained as long as the cell was depolarized, whereas average sustained calcium currents associated with this calcium rise were in all cases <2 pA and often could not be distinguished from the zero current level (Fig. 1B Left). Sustained voltage-clamp steps to potentials positive to -10 mV were associated with a transient rise in $[Ca^{2+}]_i$, but $[Ca^{2+}]_i$ decayed rapidly, often to levels below control (Fig. 1B Right). Thus there was a prominent dissociation between the evoked calcium current and $[Ca^{2+}]_i$ during sustained depolarizations in that depolarizations to potentials at which little or no macroscopic current could be measured produced substantial increases in $[Ca^{2+}]_i$, whereas sustained depolarizations to potentials that fully activated the calcium current did not result in a steady-state increase in $[Ca^{2+}]_i$.

We reasoned that the sustained rise in $[Ca^{2+}]_i$ was mediated by calcium flux through L-type calcium channel activity at the threshold of resolution, resulting in the establishment of a new equilibrium state for $[Ca^{2+}]_i$. Indeed, application of nisoldipine (20 μ M final concentration to achieve a rapid effect) immediately reversed the sustained rise in $[Ca^{2+}]_i$ associated with voltage-clamp steps within the calcium window as well as the transient rise in $[Ca^{2+}]_i$ associated with full activation of the calcium current (Fig. 2A). Moreover, the channel agonist BAY K8644 (1 μ M) shifted the calcium window to more negative potentials (Fig. 2B), consistent with its action on gating and inactivation of L-type calcium channels (21, 38). The steady-state rise in $[Ca^{2+}]_i$ associated with L-type calcium channel activity did not require amplification by calcium-induced calcium release, since ryanodine did not alter calcium responses (Fig. 3). In nine cells exposed to up to 100 μ M ryanodine, the relationship between the increase in $[Ca^{2+}]_i$ and the integrated I_{Ca} was not altered during maximal activation of the calcium current, despite the fact that exposure to ryanodine resulted in the expected gradual increase in $[Ca^{2+}]_i$.

The calcium window occurred over a voltage range between -40 and -20 mV in all cells ($n = 16$) and corresponded quite well to the window current obtained from steady-state inactivation measurements (Fig. 4), with the peak of the calcium window and the window current at approximately -30 mV. Moreover, the magnitude of the predicted window

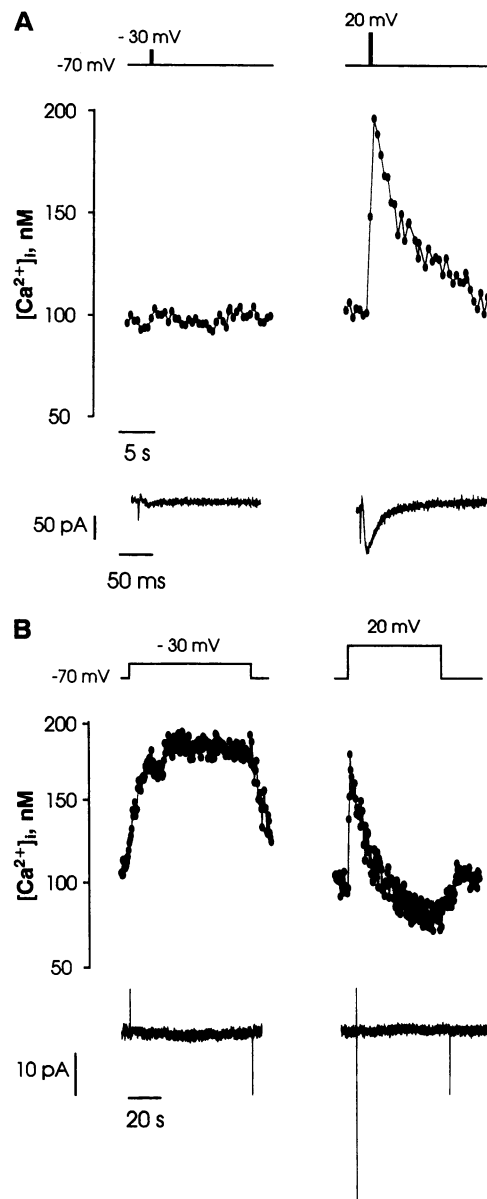


FIG. 1. Peak and steady-state calcium and current in nondialyzed, voltage-clamped myocytes. (A) The peak calcium response to 250-ms depolarizing steps is shown. Depolarization to -30 mV evoked a small calcium current that was not sufficient to achieve a measurable calcium response. Full activation of the current with a step to 20 mV resulted in a rapid rise and a slower decay in $[Ca^{2+}]_i$. (B) The response to sustained depolarizations of the same magnitude in the same cell was markedly different. Steps to -30 mV resulted in a slow rise in $[Ca^{2+}]_i$ to a steady-state level, despite the fact that a sustained macroscopic current was not resolvable. Conversely, a sustained step to 20 mV resulted in a current similar to that in A (current compressed and peak attenuated for display) and a transient rise in $[Ca^{2+}]_i$ followed by a decline below control level. Following repolarization calcium returned to control. Cell 0607.

currents obtained from measurements of the activation and steady-state inactivation of L-type calcium currents recorded under identical conditions was consistent with the magnitude of the observed steady-state currents. As shown in Fig. 4, the average predicted current magnitude at the peak of the window current was <0.5 pA. Steady-state increases in $[Ca^{2+}]_i$ in some cells were observed with steps to potentials as negative as -50 mV, consistent with recent measurements that have reported steady-state barium currents at voltages as negative as -58 mV in arterial myocytes (27). The mean

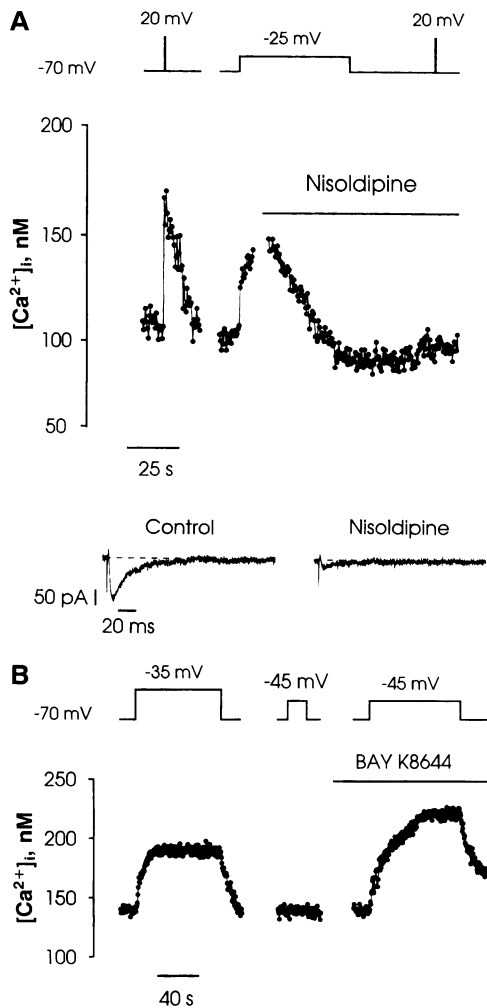


FIG. 2. Dihydropyridine-sensitive calcium channels underlie sustained rises in $[Ca^{2+}]_i$. (A) A brief (250 ms) step to 20 mV activates a calcium current and transient $[Ca^{2+}]_i$ response. Following sustained depolarization to -25 mV, $[Ca^{2+}]_i$ slowly increases toward a new steady-state. Nisoldipine ($20 \mu M$) application results in an immediate reversal of the depolarization-induced rise in calcium. A subsequent voltage clamp step to 20 mV demonstrates block of the calcium current and associated transient rise in $[Ca^{2+}]_i$. Cell 0707. (B) A sustained depolarization to -35 mV activated a steady-state increase in $[Ca^{2+}]_i$, but depolarization to -45 mV was not sufficiently positive to increase calcium. Following application of BAY K8644 ($1 \mu M$), depolarization to -45 mV evoked a larger calcium increase than occurred at -35 mV. Cell 0713. Drug applications by bath addition of 100-fold concentrated stock solutions; final ethanol concentration $<0.5\%$.

increase in $[Ca^{2+}]_i$ that occurred following sustained depolarizations to -30 mV was 97.0 ± 11.5 nM (mean \pm SEM; $n = 10$). This value is a spatial average of $[Ca^{2+}]_i$ and radial calcium gradients would be expected to result in substantially higher calcium levels at the cell periphery (37, 39). Moreover, this is likely to be a minimal estimate of the spatially averaged $[Ca^{2+}]_i$, since some attenuation of small rises in $[Ca^{2+}]_i$ by the indicator would occur even at fura-2 concentrations below $50 \mu M$ (37).

If L-type calcium channel activity underlies sustained increases in $[Ca^{2+}]_i$, then at equilibrium the calcium flux through these channels must balance calcium efflux. Using measurements of the monoexponential calcium efflux rate constant following voltage-clamp steps resulting in small perturbations in $[Ca^{2+}]_i$ (see Fig. 1), we calculated the magnitude of the steady-state calcium current required to produce a 100 nM rise in $[Ca^{2+}]_i$. When $[Ca^{2+}]_i$ achieves a

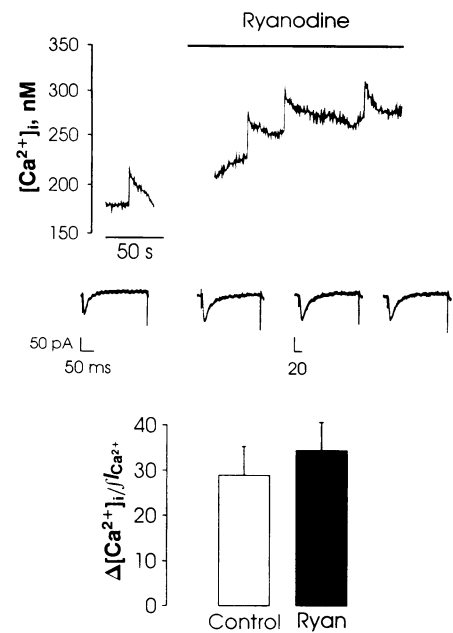


FIG. 3. Absence of evidence for calcium-induced calcium release. (Top and Middle) Step depolarizations to 10 mV were imposed before and after ryanodine ($100 \mu M$) to determine whether calcium-induced calcium release occurred; depolarizations evoked a typical rapidly inactivating current and transient rise in $[Ca^{2+}]_i$. After addition of ryanodine, $[Ca^{2+}]_i$ increased gradually, indicating an effect of the drug; calcium transients were roughly equivalent, however, before and after ryanodine exposure. (Bottom) The magnitude of the calcium transient was normalized by the integral of the calcium current for nine similar experiments in order to quantify the relationship between $\Delta[Ca^{2+}]_i$ and I_{Ca} . There was no significant difference in this relationship before and after ryanodine, as would be expected if calcium-induced calcium release were involved. Cell 0414938.

new steady state following intermediate voltage steps within the calcium window, fast $[Ca^{2+}]_i$ buffers have equilibrated and calcium influx must balance efflux by membrane pumps and other slower transport processes (37). The mass balance equation for this state is given by:

$$j_{in} = \gamma V(\Delta[Ca^{2+}]_i),$$

where j_{in} is the flux of calcium ions, γ is the combined rate constant for slow calcium efflux processes, V is the cell volume, and $\Delta[Ca^{2+}]_i$ is the increase in $[Ca^{2+}]_i$ above control. The time constant for the roughly exponential decay of calcium due to this slow buffering was on the order of 10 s, similar to previous reports (3, 40). At calcium levels well below buffer saturation, fast calcium buffering will result in a slower apparent efflux rate, and this effect will be proportional to the binding capacity of the endogenous calcium buffer (37). Correcting the observed efflux rate using measurements of the calcium binding constant obtained in nystatin-patch recordings from chromaffin cells ($k_s = 52$; ref. 36), we estimate that a steady-state calcium current of ≈ 0.5 pA would be sufficient to sustain a 100 nM increase in $[Ca^{2+}]_i$ (using a cell volume of 3 pl), consistent with the magnitude of measured macroscopic inward currents during steady-state depolarizations to a potential sufficient to produce this rise in $[Ca^{2+}]_i$ (Fig. 1B) and with the magnitude of the predicted window currents obtained from calcium current activation and steady-state inactivation measurements (Fig. 4). The underlying open-state probability of single calcium channels associated with currents on the order of 0.5 pA (assuming 1000 channels per cell and using single-channel measurements under physiological conditions; ref. 29) indicates that

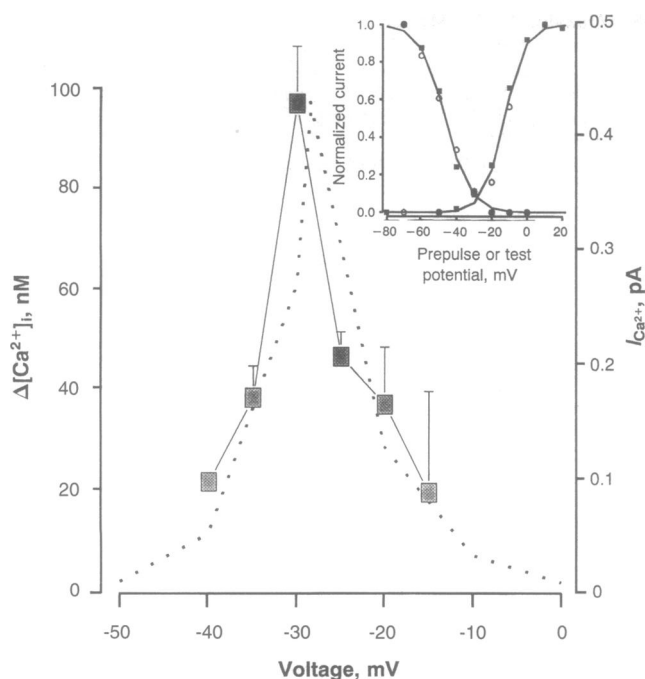


FIG. 4. Voltage-dependence of steady-state calcium window. ■, The relationship between the mean steady-state increase in $[Ca^{2+}]_i$ and the holding potential is shown for steps from -70 mV. The dotted line shows the theoretical window current from fits to calcium current activation and steady-state inactivation experiments performed under the same conditions (1.8 mM Ca^{2+} , $35^\circ C$). The window current fits have been scaled so that the peak of the current window corresponds with the peak of the mean increase in calcium. The scale at the right indicates the magnitude of the theoretical window current available at any potential, using the normalized Boltzmann values for the amount of available current and the amount of current inactivation, and the maximum available current averaged from 12 experiments (96 pA). (Inset) Full calcium current activation and inactivation experiment from two cells (symbols) and Boltzmann fit (least squares) to the data (lines).

the mean open-state probability would be ≈ 0.002 at -30 mV, roughly consistent with measurements of open-state probability near the resting potential of smooth muscle cells (28, 29). Thus voltage-dependent calcium channel activity at or below the level of detection can markedly influence $[Ca^{2+}]_i$ at resting membrane potentials.

These results emphasize the importance of the relatively slow calcium efflux kinetics of smooth muscle cells in enabling substantial increases in $[Ca^{2+}]_i$ following very modest increases in calcium channel activity. For example, the efflux rate constant of tracheal myocytes at $35^\circ C$ was more than an order of magnitude slower than that observed in cardiac cells at room temperature (4). In heart cells the Na^+/Ca^{2+} exchanger effects very rapid calcium removal, whereas membrane Ca^{2+} -ATPases underlie slower removal (4, 41). We found no evidence of Na^+/Ca^{2+} exchange; efflux rate constants determined in sodium-free solutions were equivalent to those obtained in 140 mM Na^+ and did not have the predicted voltage-dependence for the electrogenic exchanger (data not shown). Also, as shown in Fig. 3, calcium efflux rate constants were equivalent in the presence of ryanodine, suggesting that calcium removal into the sarcoplasmic reticulum (SR) does not determine the calcium efflux kinetics of voltage-dependent calcium influx. While the kinetics of calcium removal in our experiments are most consistent with calcium efflux associated with sarcolemmal ATPase activity (4, 41), we cannot exclude some uptake into the fully loaded SR.

In summary, these measurements suggest two mechanisms by which voltage-dependent calcium channels regulate $[Ca^{2+}]_i$: (i) action potentials evoke large transient increases in

$[Ca^{2+}]_i$ that decay with a time constant on the order of the interspike interval (4, 7, 40), resulting in rises in $[Ca^{2+}]_i$ that depend on action potential frequency; and (ii) sustained depolarizations result in sustained rises in calcium over a limited voltage range, despite the fact that macroscopic currents are not detectable. This latter mechanism is likely to be of greater importance in tonic smooth muscle cells and nonexcitable cells that have stable resting membrane potentials and express L-type calcium channels.

We thank Drs. M. Welsh, F. Fay, M. Nelson, and M. Pring for helpful suggestions and Ms. Kim Bailey for technical assistance. This research was supported by National Institutes of Health Grant HL-45239 (M.I.K.).

- Gorman, A. L. F. & Thomas, M. V. (1980) *J. Physiol. (London)* **308**, 259–285.
- Augustine, G. J., Charlton, M. P. & Smith, S. J. (1985) *J. Physiol. (London)* **367**, 143–162.
- Becker, P. L., Singer, J. J., Walsh, J. V., Jr., & Fay, F. S. (1989) *Science* **244**, 211–214.
- Wier, W. G. (1990) *Annu. Rev. Physiol.* **52**, 467–485.
- Tsien, R. W. & Tsien, T. Y. (1990) *Annu. Rev. Cell Biol.* **6**, 715–760.
- Hille, B. (1992) *Ionic Channels of Excitable Membranes* (Sinauer, Sunderland, MA).
- Miller, R. J. (1991) *Prog. Neurobiol.* **37**, 255–285.
- Fabiato, A. (1983) *Am. J. Physiol.* **245**, C1–C14.
- Cannell, M. B., Berlin, J. R. & Lederer, W. J. (1987) *Science* **238**, 1419–1423.
- Callewaert, G., Cleemann, L. & Morad, M. (1988) *Proc. Natl. Acad. Sci. USA* **85**, 2009–2013.
- Talo, A., Stern, M. D., Spurgeon, H. A., Isenberg, G. & Lakatta, E. G. (1990) *J. Gen. Physiol.* **96**, 1085–1103.
- Draznin, B., Sussman, K., Kao, M., Lewis, D. & Sherman, N. (1987) *J. Biol. Chem.* **262**, 14385–14388.
- Nelson, M. T., Standen, N. B., Brayden, J. E. & Worley, J. F. (1988) *Nature (London)* **336**, 382–385.
- McCarty, N. A. & O'Neil, R. G. (1990) *Am. J. Physiol.* **259**, F950–F960.
- Cavalié, A., Ochi, R., Pelzer, D. & Trautwein, W. (1983) *Pflügers Arch.* **398**, 284–297.
- Mitchell, M. R., Powell, T., Terrar, D. A. & Twist, V. W. (1983) *Proc. R. Soc. London B* **219**, 447–469.
- Josephson, I. R., Sanchez-Chapula, J. & Brown, A. M. (1984) *Circul. Res.* **54**, 144–156.
- Kass, R. S. & Sanguinetti, M. C. (1984) *J. Gen. Physiol.* **84**, 705–726.
- Lee, K. S., Marban, E. & Tsien, R. W. (1985) *J. Physiol. (London)* **364**, 395–411.
- McDonald, T. F., Cavalié, A., Trautwein, W. & Pelzer, D. (1986) *Pflügers Arch.* **406**, 437–448.
- Cohen, N. M. & Lederer, W. J. (1987) *J. Physiol. (London)* **391**, 169–191.
- Langton, P. D., Burke, E. P. & Sanders, K. M. (1989) *Am. J. Physiol.* **257**, C451–C460.
- Imaizumi, Y., Muraki, K., Takeda, M. & Watanabe, M. (1989) *Am. J. Physiol.* **256**, C880–C885.
- Smirnov, S. V. & Aaronson, P. I. (1992) *J. Physiol. (London)* **457**, 455–475.
- Hirano, Y., Moscucci, A. & January, C. T. (1992) *Circul. Res.* **70**, 445–455.
- Scherubl, H. & Hescheler, J. (1991) *Proc. R. Soc. London B* **245**, 127–131.
- Langton, P. D. & Standen, N. B. (1993) *J. Physiol. (London)* **469**, 535–548.
- Nelson, M. T., Patlak, J. B., Worley, J. F. & Standen, N. B. (1990) *Am. J. Physiol.* **259**, C3–C18.
- Gollasch, M., Hescheler, J., Quayle, J., Patlak, J. B. & Nelson, M. T. (1992) *Am. J. Physiol.* **263**, C948–C952.
- Fleischmann, B. K., Washabau, R. J. & Kotlikoff, M. I. (1993) *J. Physiol. (London)* **468**, 625–638.
- Gryniewicz, G., Poenie, M. & Tsien, R. Y. (1985) *J. Biol. Chem.* **260**, 3440–3450.
- Kajita, J. & Yamaguchi, H. (1993) *Am. J. Physiol.* **264**, L496–L503.
- Korn, S. J. & Horn, R. (1989) *J. Gen. Physiol.* **94**, 789–812.

34. Hamill, O. P., Marty, A., Neher, E., Sakmann, B. & Sigworth, F. J. (1981) *Pflügers Arch.* **391**, 85–100.
35. Scanlon, M., Williams, D. A. & Fay, F. S. (1987) *J. Biol. Chem.* **262**, 6308–6312.
36. Zhou, Z. & Neher, E. (1993) *J. Physiol. (London)* **469**, 245–273.
37. Neher, E. & Augustine, G. J. (1992) *J. Physiol. (London)* **450**, 273–301.
38. Quayle, J. M., McCarron, J. G., Asbury, J. R. & Nelson, M. T. (1993) *Am. J. Physiol.* **264**, H470–H478.
39. Lipscombe, D., Madison, D. V., Poenie, M., Reuter, H., Tsien, R. W. & Tsien, R. Y. (1988) *Neuron* **1**, 355–365.
40. Ganitkevich, V. Y. & Isenberg, G. (1991) *J. Physiol. (London)* **435**, 187–205.
41. Carafoli, E. (1988) *Methods Enzymol.* **157**, 3–11.